The value of fusion energy to a decarbonized United States electric grid

Jacob A. Schwartz[a,1,*], Wilson Ricks[b], Egemen Kolemen[a,b,c,*], Jesse D. Jenkins[b,c]

[a] *Princeton Plasma Physics Laboratory, 100 Stellarator Rd, Princeton, 08543, New Jersey, United States of America*
[b] *Department of Mechanical and Aerospace Engineering, Princeton University, Olden St., Princeton, 08540, New Jersey, United States of America*
[c] *Andlinger Center for Energy and the Environment, Olden St., Princeton, 08540, New Jersey, United States of America*

Summary

Fusion could be a part of future decarbonized electricity systems, but it will need to compete with other technologies. In particular, pulsed tokamak plants have a unique operational mode, and evaluating which characteristics make them economically competitive can help select between design pathways. Using a capacity expansion and operations model, we determined cost thresholds for pulsed tokamaks to reach a range of penetration levels in a future decarbonized US Eastern Interconnection. The required capital cost to reach a fusion capacity of 100 GW varied from \$3000 to \$7200 kW^{-1}, and the equilibrium penetration increases rapidly with decreasing cost. The value per unit power capacity depends on the variable operational cost and on the cost of its competition, particularly fission, much more than on the pulse cycle parameters. These findings can therefore provide initial cost targets for fusion more generally in the United States.

Keywords: nuclear fusion, tokamaks, capacity expansion, technology assessment

1. Introduction

Technology for the production of electrical power via nuclear fusion is under development by governments and private companies around the world [1]. In fusion reactors, light atomic nuclei undergo exothermic reactions in a hot plasma, and the kinetic energy of the products heats a working fluid [2] or is converted directly to electrical energy [3]. Fusion would be a firm energy resource [4] without

*Corresponding author
Email addresses: jacobas@princeton.edu (Jacob A. Schwartz), ekolemen@princeton.edu (Egemen Kolemen)
[1] Lead contact

operational CO_2 emissions, and could contribute to the deep decarbonization of the electricity sector in the United States and elsewhere. However, even if fusion's physics and engineering challenges are overcome, there are many other technologies for electricity production. Fusion will need to compete economically with these other technologies in order to be part of the US energy mix. Within fusion itself there are multiple reactor concepts, with wide plausible ranges for operational parameters. While it is difficult to determine the cost of a particular design when much of the underlying technology has yet to be developed, it is possible to set cost targets by determining the value of a design with a particular set of operational parameters in a simulated future electricity system. This value-driven approach[5–7] can help to determine which fusion concepts or technology pathways would be most useful when deployed alongside future competing and complementary energy technologies.

There have been general studies on markets for fusion energy[8], on fusion costing[9,10], its integration into energy systems[11], and on the value of fusion for future electricity systems in Europe[12]. However, this work is the first in which plants with fusion-specific operational constraints have been integrated into a temporally-resolved system-scale model. This allows for investigation of the costs of these constraints and of how fusion interacts with other resources on an hour-by-hour basis. This is also the first study of the equilibrium value of fusion at various levels of capacity penetration for the United States, and the first investigation of the value of integrated thermal storage for fusion plants in an hourly model.

In this study we used GenX, an electricity system capacity expansion model, to capture the operational and economic interactions between fusion plants and a number of competing energy technologies in simulated future electricity systems[13]. GenX is a linear optimization model that identifies an optimal set of energy technology deployment, retirement, and operational decisions to minimize total electricity system cost over a specified planning horizon. As is done in real power systems, GenX solves an 'economic dispatch'[14] problem that dispatches grid assets so as to minimize the cost of exactly meeting electricity demand at every hour over the course of a modeled year, subject to a number of operational constraints. GenX and similar capacity expansion models also capture the declining value of energy technologies with increasing deployment, arriving at a long-run economic equilibrium in which each non-constrained technology's marginal cost equals its marginal value to the system. This reflects the assumption that an effective central planner will only make investments that reduce the total cost of serving electricity demand, or equivalently that developers in a deregulated market will continue to deploy a given technology until marginal capacity additions become unprofitable. Capturing both these short- and long-run system-level interactions is necessary in order to accurately assess market sizes and cost targets for an emerging energy technology like fusion.

There are multiple existing concepts for fusion power plants, including pulsed[15–17] and steady-state[18] tokamaks, stellarators[19–21], laser-driven inertial confinement devices[22,23], magnetized target fusion systems[24,25], mirror machines[26], field-reversed configurations[27], and Z-pinches[28,29]. For the present study we devel-

oped an abstracted operational model for a fusion plant using a pulsed tokamak design that could be linearized and implemented in GenX (see Sections 2 and Note S3). The tokamak was chosen because it is the most mature fusion concept—ITER[30], DEMO[31], and one of the largest private fusion companies employ it—and because it has the most general set of performance characteristics when examined with hourly resolution.

Tokamaks confine a hot plasma in a toroidal chamber using magnetic fields, some externally imposed, and some produced by an electric current flowing through the plasma. Pulsed tokamaks use magnetic induction from a component called the central solenoid[32] (CS) to drive this current. During the 'flat-top' of the plasma pulse, which is typically designed to last half an hour[33] to several hours[31], a constant rate of change in magnetic flux in the CS drives a constant voltage (and current) in the plasma. The flat-top is when most of the fusion occurs, which generates heat. The CS has a maximum magnetic flux that it can hold, and the plasma cannot be sustained without a driving voltage, so the flat-top must end. During the following 'dwell period', typically a fraction of an hour, the solenoid and other systems are reset, and no fusion occurs. Restarting the plasma requires significant electrical power, with peak levels, for seconds or minutes, comparable to the output capacity of the plant[34], which would likely be buffered by some storage on-site. The net output of the plant therefore varies over the pulse cycle. While this study focuses on pulsed tokamaks, the range of performance characteristics considered can represent a wide range of potential alternative concepts.

We used the fusion model as implemented in GenX to study the value and role of fusion power in a decarbonized US Eastern Interconnection circa the 2040s, optimizing electricity technology investments and hourly operations across 20 model zones to minimize total system cost. In order to understand the design space of model tokamaks, we varied their behavior from pulsed to nearly steady-state, and varied the variable operations and maintenance cost to reflect uncertainty in the costs of replaceable components such as the blanket and divertor. We explored the inclusion of integrated thermal storage with a range of capacity costs, and we varied assumptions about the cost and availability of other resources to understand the sensitivity of fusion's value to these market uncertainties and how fusion interacts with these resources. In the present work we optimized the electricity system with respect to an exogenously fixed total fusion capacity, using GenX outputs to calculate the cost threshold at which fusion could achieve this level of deployment. See the Methods section for a more detailed description of the procedure used to identify cost thresholds. The GenX model as configured for this study includes the following constraints:

- zero direct carbon emissions from electricity system operations;
- a 'capacity reserve margin' policy to ensure sufficient generation capacity in a number of reliability regions;
- supply curves reflecting resource constraints on solar and wind power in each zone;

Figure 1: [Model fusion plant composition and operation.] Part (a): Fusion plant diagram. Parts (b) and (c) show qualitatively the unresolved, sub-hourly structure of the plasma pulse and recirculating power flows in the pulsed tokamak fusion core. These plots provide one interpretation for the mathematical models implemented; in reality there would be additional structure and detail[34]. Part (b) plots the $p_{\mathrm{core,th}}$, the thermal power generated by a core with a total pulse cycle time $t_{\mathrm{pu}} = 2\,\mathrm{h}$ and a dwell time $t_{\mathrm{dw}} = 0.5\,\mathrm{h}$. It also shows, in gray, the gross hourly electric power generated if thermal storage is not employed, $p^{\mathrm{binned}}_{\mathrm{gross,el}}$. Part (c) shows the three types of recirculating power: passive, active and the startup power. The associated startup energy fraction is also labeled, e_{start}.

- operational constraints for thermal generators that specify a minimum output level while committed, limits on how often plants can cycle on or off, and maximum power ramp rates;
- limits on the expansion of transmission lines between zones and losses when power is transmitted between zones;
- a fusion reactor core which can operate flexibly, without limits on thermal cycling;
- no maintenance scheduling or unscheduled outages for fusion nor other resources;
- no other specific policies, subsidies or external regulations.

Across a range of fusion plant designs and market scenarios, we find that reaching 100 GW of fusion capacity (which is about 10% of the peak demand, and similar to the present-day US fission fleet capacity) requires that the capital cost of the plant falls below \$3000/kW to \$7200/kW of net electric output capacity. Roughly half of this range results from the space of internal fusion operational parameters, and half from uncertainty in the cost and performance of competing generation and storage technologies in future electricity markets. The former half can be mostly attributed to the variation in the marginal cost of net generation, rather than to the variation in operational constraints such as the pulse length. This implies that the results should generalize from pulsed tokamaks to other concepts, and simplifies prediction of the value of a design in a given scenario. Between scenarios, the value of fusion differs in large part because of the differing costs of fission, and fusion's competition with other resources becomes significant only after fission has been displaced. Including the option to build thermal storage increases the value of the fusion core by up to \$1000/kW, and in some scenarios, adding thermal storage increases the relative value of solar and wind.

2. A representation of pulsed tokamaks for electricity systems modeling

For this study we developed a fusion plant model for integration into GenX. Figure 1 part (a) illustrates the modeled components of the plant. There are

three parts: a fusion core which takes in parasitic 'recirculating' power from the grid and makes heat, an (optional) thermal storage system (TSS), which stores heat between hourly periods, and a power conversion system (PCS) that takes heat from the core or the TSS and generates electricity for the grid.

Parts (b) and (c) illustrate the operation of the core which is then binned into hourly increments. The core operates on cycles of length t_{pu}, an integer number of hours. During the first hourly period it rests for the 'dwell period' t_{dw}, a fraction of an hour during which time it generates no heat. Plasma ramp-up and ramp-down periods are not explicitly accounted for since they are typically much shorter than an hour; these could be modeled by adjusting the length of the dwell period. While the core is operating it generates a peak thermal power $p_{\mathrm{core,th}}$. This corresponds to a peak gross electric power $p_{\mathrm{gross,el}} = \eta^{discharge} p_{\mathrm{core,th}}$ where $\eta^{discharge}$ is the thermal efficiency of the PCS. If there is no thermal storage system, the heat generated in an hourly period must be converted to electrical energy during the same period; the gross electric power $p^{\mathrm{binned}}_{\mathrm{gross,el}}$ therefore varies from hour to hour.

The recirculating electrical power, shown in (c), is described by four dimensionless parameters which denote fractions of the peak gross electric power: r_{pass}, r_{act}, e_{start}, and r_{start}. The passive recirculating power $r_{\mathrm{pass}} p_{\mathrm{gross,el}}$ is drawn regardless of the core's status, the active recirculating power $r_{\mathrm{act}} p_{\mathrm{gross,el}}$ is drawn proportionally to the fraction of the hour during which the core operates, and the start energy $e_{\mathrm{start}} p_{\mathrm{gross,el}}$ h (where h is one hour) is a fixed quantity required for each core start. The start power level $r_{\mathrm{start}} p_{\mathrm{gross,el}}$ models a brief peak power draw from outside the plant. It does not enter into the recirculating power calculation; rather, spare power capacity must be available in the same zone during the hour that the core starts.

A final parameter for the core is $\pi^{VOM,th}$, the variable operations and maintenance (OM) cost of generating a quantity of heat from the core. This represents the cost of replacements for the blanket and divertor, which are assumed to need replacement after being bombarded with a certain quantity of neutrons; neutron exposure is proportional to heat generated in the core. Damage due to accumulation of thermal cyclic fatigue is not explicitly modeled. However, since the fusion plants generally operate near their peak capacity, costs of thermal cyclic fatigue accumulated during successively-pulsed operation could be incorporated into the variable operational cost.

The PCS has five main parameters: the thermal efficiency $\eta^{discharge}$; the capital cost π^{invest}; the fixed OM cost π^{FOM}; and the variable OM cost π^{VOM}, which is accrued in proportion to the gross electric power generated; and the minimum output level ρ^{min}. The thermal storage system (TSS) has only one parameter, the storage capacity investment cost, which is varied between specific cases. For simplicity, we assume no efficiency losses associated with the thermal storage, nor costs associated specifically with maximum inflow or outflow rates.

From the parameters of the core and PCS, one can calculate several derived quantities: f_{active}, the fraction of the time that the core can be active; $f_{\mathrm{netavgcap}}$, the ratio of the time-averaged net electric power produced to the gross electric power generation capacity; f_{recirc}, the fraction of the gross electric power which

Table 1: Reference pulsed tokamak models used for this study.

	Pessimistic	Mid-range	Optimistic	
Core parameters				
t_{pu}	2	4	1	h
t_{dw}	0.15	0.15	0.063	h
r_{act}	0.2	0.1	0.014	
r_{pass}	0.2	0.1	0.027	
r_{start}	0.2	0.1	0	
e_{start}	0.05	0.025	0	
$\pi^{VOM,th}$	5	3	1	$/MWh$_{\mathrm{th}}$
Power conversion system parameters				
$\eta^{discharge}$		0.4		
ρ^{min}		0.4		
π^{invest}		750		$/kW$_{\mathrm{e}}$
π^{FOM}		18.75		$/kW$_{\mathrm{e}}$yr
π^{VOM}		1.74		$/MWh$_{\mathrm{e}}$
Derived quantities				
f_{active}	0.925	0.9625	0.9375	
$f_{\mathrm{netavgcap}}$	0.515	0.76	0.897	
f_{recirc}	0.44	0.21	0.043	
Q_{eng}	1.26	3.76	22.4	
$\pi^{VOM,total}$	26	12	4.4	$/MWh$_{\mathrm{e}}$

is used by the plant itself; Q_{eng}, the ratio of the net power output to the recirculating power; and $\pi^{VOM,total}$, the total cost of generating a unit of net electrical energy. Formulas for these are given in the Methods section.

The fusion plants in this study are based on one of three reference designs, listed in Table 1. These are labeled pessimistic, mid-range, and optimistic, based on their core parameters and especially their resulting VOM cost $\pi^{VOM,total}$. The pessimistic plant requires a large dwell time between pulses, about 44% of the gross electric power generated is required to operate the plant [34,35], and the marginal cost of net energy generation $\pi^{VOM,total}$ is \$26/(MW h), closer to that of a natural gas plant with carbon capture and storage (NG-CCS) than that of a fission plant.

The optimistic plant has a shorter dwell time, recirculating power levels tenfold lower, and has less costly operation at \$4.4/(MW h), half that of fission plants. A mid-range design has pulse cycle parameters, recirculating power, and marginal costs of net generation roughly halfway between the optimistic and pessimistic designs.

All plants share the same PCS design. The assumed capital cost of \$750/kW is a 28% reduction, based on an economy of scale, from the 'Power cycle' cost of the Molten Salt Power Tower in the 2018 NREL System Advisor Model [36]: see Table 3 of Turchi [37]. The thermal conversion efficiency is $\eta^{discharge} = 0.4$,

and the variable operations and maintenance cost $\pi^{VOM} = \$1.74/(\mathrm{MW\,h})$.

The annual fixed OM cost is assumed to be 2.5% of the capital cost; the same assumption is made for the TSS and the core itself.

3. Cost targets for fusion plants without integrated thermal storage

We determined cost thresholds as function of capacity penetration for the three reference plants in three main scenarios. The three scenarios, termed low, medium, and high fusion market opportunity, differ in the cost of the available resources, which are: solar photovoltaics (PV), on- and off-shore wind, fission, natural gas plants with 100% carbon capture and storage (NG-CCS), plants burning a zero-carbon fuel such as hydrogen or biomethane in a combined cycle or combustion turbine (ZCF-CC or ZCF-CT, respectively), lithium-ion batteries and metal-air batteries. The investment costs and operational costs of these resources, listed in Tables 2 and 3, respectively, are lowest in the low market opportunity scenario and highest in the high market opportunity scenario. All the scenarios have identical nominal loads, with average and peak values of 600 GW and 1100 GW, respectively. One difference is in the quantity of certain loads, representing electric vehicle charging and residential hot water-heaters, which can be shifted in time by a few hours: for example, in the low, medium, and high market opportunity scenarios, 0.9, 0.75, and 0.6, respectively, of the vehicle charging loads can be delayed by up to 5 hours. See Table S2 for full details. The three scenarios do not differ in the costs or maximum procurable quantities of inter-regional transmission. In the high market opportunity scenario, fission is not built because it is too expensive, and nearly the maximum amount of transmission is required for the resulting renewables-dominated grid. In cases in medium and low market opportunity scenarios without fusion, there is about 100 GW of fission (see also Figs S35 and S36) and the grid is less limited by transmission constraints.

Figure 2 shows the cost thresholds for a marginal plant for each plant design in each scenario, as the fusion capacity penetration is set from 10 GW to 350 GW. In equilibrium, the capital cost of a plant built to reach a specified total installed capacity must be equal to or lower than this respective curve. For a fixed fusion capacity, the cost targets differ between plant designs as much as they differ between the three market opportunity scenarios. For many of the curves a small cost decrease leads to much wider adoption: for the mid-range reactor in the medium opportunity scenario, the two bold points show where a cost decrease of \$500/kW increases the equilibrium fusion capacity from 10 GW to 100 GW. This suggests that if the initial cost targets can be met, even shallow learning curves could lead to a significant fusion capacity.

4. Internal and external drivers of value

Within a given market opportunity scenario, the difference in value between these pulsed tokamak designs is driven by the difference in the marginal cost

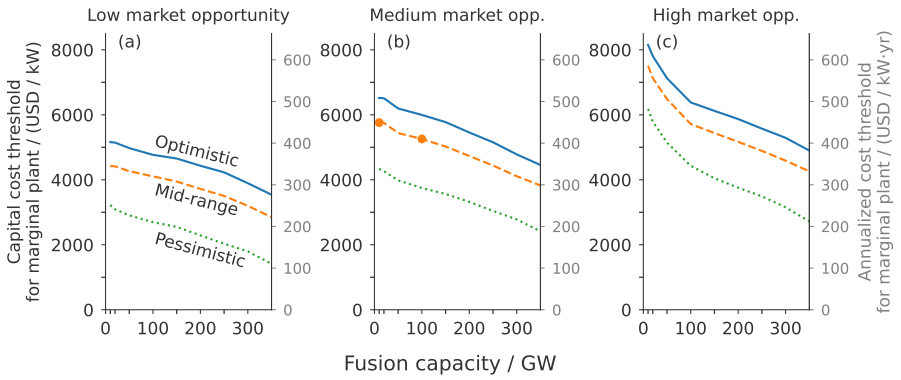

Figure 2: [Cost thresholds for a marginal unit of fusion capacity as a function of the total installed fusion capacity.] The cost threshold for a marginal unit of fusion capacity corresponds to the maximum break-even capital cost for the final fusion plant built to reach a specified total installed capacity. Results are presented for three reference reactors without integrated thermal storage and in the three market opportunity scenarios. Annualized costs are 7.8% of the capital cost per year: see Note S2 for details. The two bold points on the mid-range core, medium market opportunity scenario curve highlight how a decrease in capital cost of \$500/kW can increase the capacity penetration from 10 GW to 100 GW. See Figure S9 for cost thresholds in additional scenarios.

of net generation $\pi^{VOM,total}$, and between market opportunity scenarios, by differences in the costs of competitor resources.

Figure 3(a) plots the three reference plants, along with a gray line representing a set of idealized plants with no recirculating power or pulse constraints, but finite VOM costs. All three reference plants lie close to this curve, which demonstrates that the penalty of pulsed operation is small. The mid-range plant value (orange star) is just 0.6% below that of the idealized plant with the same marginal cost of net generation; the pessimistic plant value (green square) is about 6% lower than that of the equivalent. Its deviation from the curve is driven largely by the core start power constraint.

Parts (b) and (c) examine the variation in the value of the mid-range plant as its operational parameters are modified, one at a time, over ranges shown in the table. After $\pi^{VOM,th}$, the two parameters with the largest effect are the passive and active recirculating power fractions. The slopes of these are nearly the same as the slope of the curve formed by modifying $\pi^{VOM,th}$. This indicates that these parameters have altered the plant value primarily through changing the marginal cost of net generation. Modifying the other quantities yields variations in plant value of less than 3%. When the pulse length is changed from 4 hours to 1 hour the value decreases due to the increased marginal cost of net generation, and also due to the increased quantity of power which must be drawn from the grid; the same value decrease is observed when quadrupling the core start power at the original pulse length. Since within a given scenario the plant value is predicted almost entirely by the cost of marginal generation, our

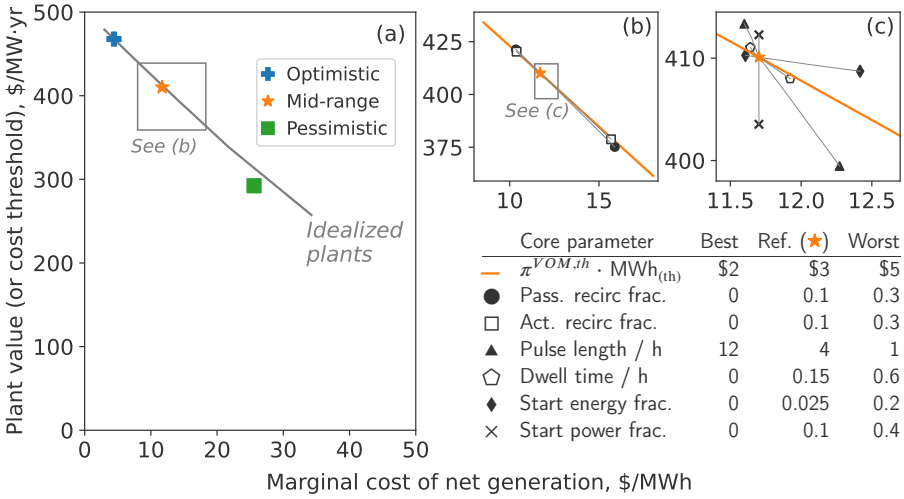

Figure 3: [Influence of plant operational parameters on the marginal value of fusion.] Part (a): The marginal value of fusion plants at 100 GW of capacity in the medium market opportunity scenario are shown as a function of their marginal cost of net generation. The gray line shows the values of a set of plants with an idealized fusion core, which has no pulse constraints or recirculating power, but finite VOM costs. Parts (b) and (c): as the parameters of a plant with a mid-range fusion core are altered from their reference values, one at a time, variation in plant value is largely due to the variation in the marginal cost of net generation, shown by the orange line. The table lists the ranges over which the parameters were varied. The unitless parameters are specified as fractions of the plant's peak gross electric power; see the Section 2.

studies should be applicable to assess the value of a wide range of devices, not only pulsed tokamaks, as part of similar future electricity systems. Given this finding, much of the further study focuses on plants like the mid-range reference plant with a modified $\pi^{VOM,th}$.

The marginal value of fusion is determined by the resources that it competes with or complements, and the composition of this set depends on the $\pi^{VOM,total}$ of a given fusion plant. Figure 4 shows how the cost thresholds for fusion at various capacity penetrations vary between the three main scenarios with the cost of other resources. Particularly at low fusion capacity penetrations, the cost of fission strongly affects the potential value of fusion: in order for a fusion plant with a similar $\pi^{VOM,total}$ to that of fission to be built, it must have a lower capacity cost. Note that a significant penetration of fusion is not guaranteed even if neither fission nor natural gas with carbon capture and storage is available: in additional scenarios with neither (see Fig. S14) fusion competes with a combination of renewables, storage, and peaker plants burning zero-carbon fuels, with the last acting as a firm generator.

Figure 5 shows explicitly that (in the medium market opportunity scenario) fission is the first competitor for any of the three reference plants. In terms of annual energy production, all three primarily substitute for fission until 100 GW when the latter is fully displaced. Afterward, plants with the optimistic design displace mainly solar, wind, and batteries, while the pessimistic plant substitutes for more NG-CCS than solar. In systems with fusion plants of the pessimistic design, slightly more solar is built at low fusion capacity penetrations, as recirculating power can be drawn from solar that would have been curtailed. Integrated thermal storage for fusion plants, discussed in the next section, further increases the value of solar and decreases the value of other resources—see also Figs. S10–S13.

5. Value of plants with thermal storage

Pulsed tokamak designs may require[39] an integrated thermal storage system (TSS) to supply the power conversion system (PCS) with heat during the dwell period; the PCS typically cannot handle the sudden decline in heat production associated with the end of the fusion pulse. However, these systems only store a few core-minutes of heat. We studied the value of adding an inter-hourly TSS with energy capacity costs similar to those of molten salt between the fusion core and PCS. We independently optimize the core capacity, storage energy capacity, and PCS generation capacity in each model zone. This allows for generators to be oversized relative to their fusion cores, in order to generate more energy during the most valuable time periods, such as periods of peak demand and/or minimal wind and solar availability. This section describes the increase in the value of the core with the option to build storage, and Section 7 describes changes in operational patterns for a plant with storage.

Figure 6 shows the increase in the equilibrium value of the fusion core with operational parameters like that of the mid-range reference plant, per unit of capacity, as functions of the marginal cost of net generation $\pi^{VOM,total}$ and

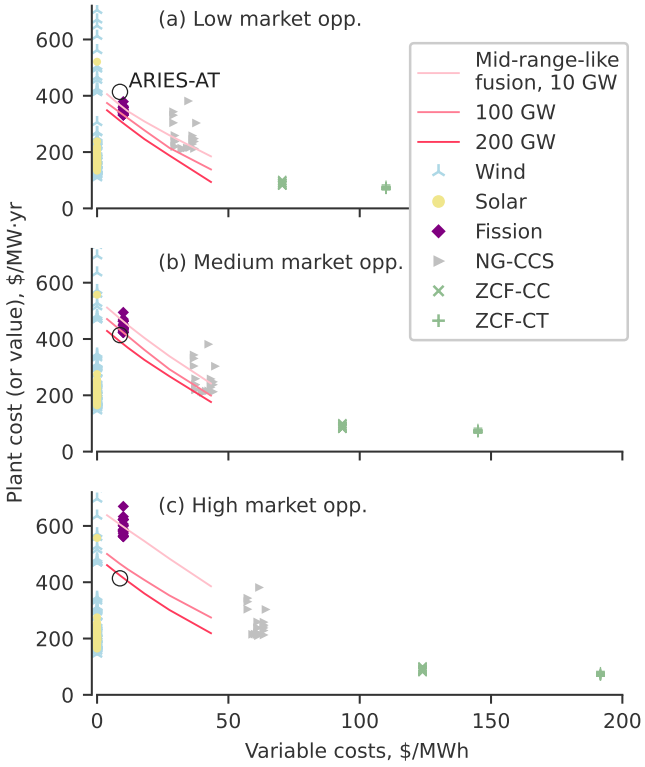

Figure 4: [The value of fusion compared with the costs of competitor resources.] For a given fusion plant design, differences in its value between scenarios depends largely on the costs of competitor resources. Cost thresholds to reach three capacity penetration levels for mid-range-like fusion plants are shown alongside the costs of other resources. These plants have the operational constraints of the mid-range reference plant but altered variable costs. Resource costs are plotted separately for each geographic zone and costs of solar and wind are normalized by their annual availability. NG-CCS are plants burning natural gas with carbon capture and storage. ZCF-CC and -CT are combined cycle and combustion turbine plants, respectively, burning zero-carbon fuels. A marker for the ARIES-AT fusion plant study [38] is provided for comparison. See Figure S14 for cost and value data in the variant scenarios.

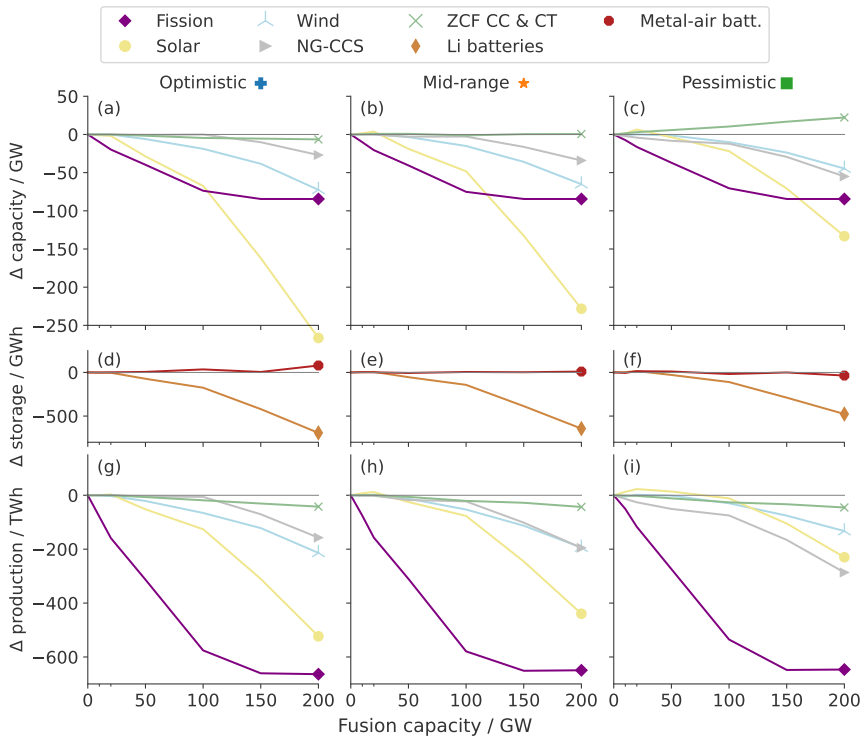

Figure 5: [Competition between fusion and other resources.] Altered generation capacity, storage capacity, and annual energy production of competitor resources as a function of fusion's capacity penetration, in sets of cases for each of the three reference fusion plants, for the medium market opportunity scenario. See also Figure S19 for the absolute quantities of each resource in this scenario, Figures S15–S24 for those in other scenarios, and Figures S25–S34 for altered quantities in other scenarios.

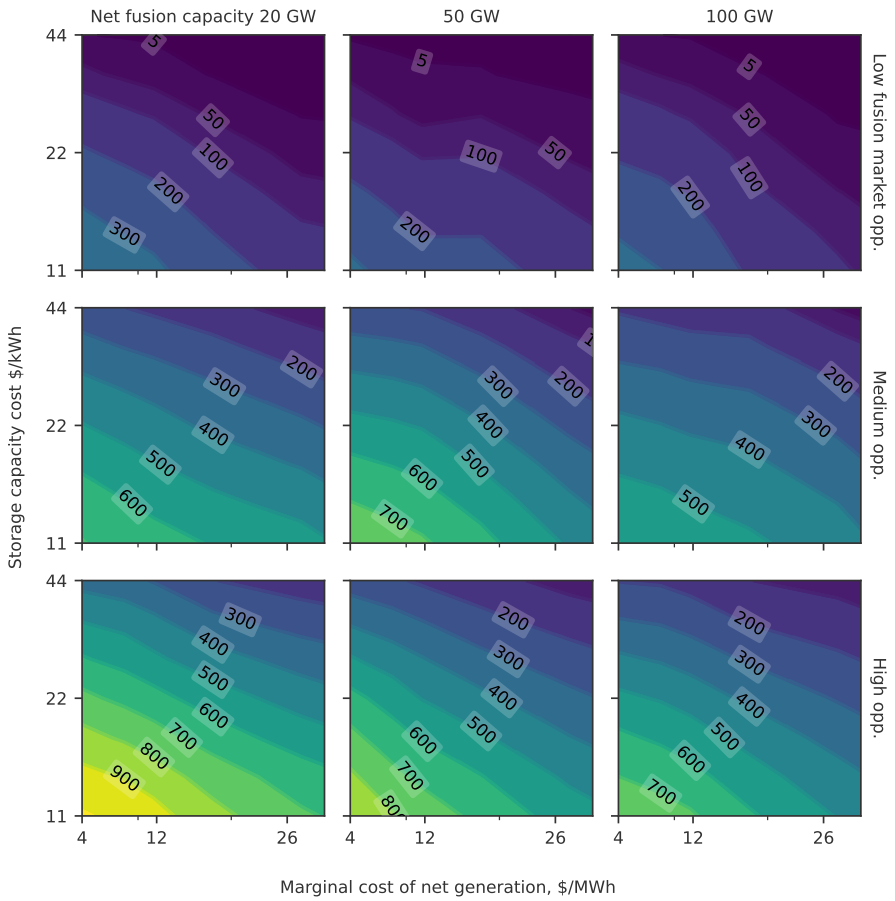

Figure 6: [Additional value associated with integrated thermal storage.] The option to build integrated thermal storage increases the value of fusion. Contours show the increase in the break-even price per unit of capacity for a mid-range-like fusion core to reach the given equilibrium penetration level, in $/kW. The plant's marginal cost of net generation $\pi^{VOM,total}$ is varied as a proxy for variation between the three reference cores. See Figures. S10–S13 for data on the total core value, optimal storage duration, and optimal PCS size.

the storage capacity cost. Especially for plants in the medium and high fusion opportunity scenarios, this is a substantial increase in the threshold capital cost for the plant core. For example, adding TSS at a cost of \$22/kW$_{th}$ increases the value of a mid-range fusion plant's core at 50 GW of penetration by \$490/kW, or about 10%. The option to build storage is more valuable at lower fusion capacity penetrations because the optimal storage quantity per plant is larger. This suggests that a TSS could be especially valuable for the first generation of fusion plants. As fusion penetration increases and the total thermal storage capacity along with it, the marginal value per unit of additional storage capacity declines.

The optimal thermal storage system (TSS) duration (Fig. S10) generally ranges from 2 h to 8 h, depending foremost on the storage capacity cost, and the optimized PCS capacity (Fig. S11) generally ranges from 1.1 to 1.35 times the amount needed to serve the fusion cores without storage. The durations are suitable for diurnal storage and allow the PCS to supply increased power during the night, when the lack of solar power production and overnight demand from EV charging and electric heat pumps makes electricity more valuable in this deeply decarbonized energy system.

6. Capacity factors and the value of flexibility

In grids dominated by variable renewables like those in this study, the electricity price is often zero (in the base cases without fusion, 10-50% of the year, depending on the scenario and geographic zone); generating electricity from fusion during these hours is not profitable. As shown in Section 4, an increased variable operations and maintenance (VOM) cost decreases the marginal value of a plant. Plants with a higher VOM cost are run less frequently, as under economic dispatch they are typically only called on to generate when electricity demand is high and plants with lower variable operating costs are already generating at maximum capacity. Figure 7, parts (a) through (c), show the capacity factor—the ratio of the fusion plants' annual net output to their maximum possible net output—for mid-range-like plants without thermal storage systems in the three market opportunity scenarios, and for three levels of capacity penetration. For the 10 GW level in the low and medium market opportunity scenarios, a stepwise decrease in capacity factor occurs if the VOM cost exceeds the variable operating cost of the fission plants. The capacity factor for the fleet can increase with penetration, as fusion displaces fission.

In plants with passive recirculating power, the capacity factor of the core is higher than that of the overall plant. In Medium market opportunity cases with 50 GW of fusion, the annual capacity factors of the fusion plants (cores) are 90% (90%), 84% (86%), or 73% (81%), for plants of optimistic, mid-range, or pessimistic designs, respectively.

Although fusion plants have generally been considered as 'baseload' plants that run continuously, dispatchable operation (the ability to turn on and off, or otherwise modulate their power output) adds to their value. In scenarios where we force fusion plants of the three reference designs to operate at full capacity

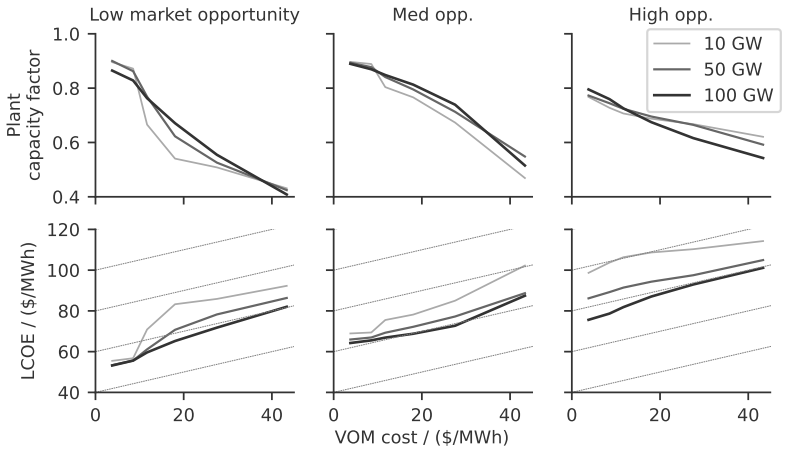

Figure 7: [Fusion plant capacity factors and LCOE.] Top row: capacity factors for mid-range-like plants with varying VOM costs in the three market opportunity scenarios, for three levels of capacity penetration, and without a TSS. Bottom row: computed 'cost of electricity' metrics for the same plants, taking into account their capacity factor. Dashed lines with a slope of 0.5 guide the eye.

year-round, their marginal break-even cost decreases by \$50/kW, \$130/kW, and \$340/kW, respectively, as they accumulate operational costs during periods of low prices. This loss of value is especially important for plants with high VOM costs which already have a lower capital cost threshold.

Thermal storage increases the capacity factor of the plants and modifies the operational patterns of the cores and PCSs. In equivalent cases in the same scenario, adding the option to build thermal storage for \$22/kWh$_{\mathrm{th}}$ increases the capacity factors of the plants (core) to 98.4% (98.6%), 94.7% (95.5%), and 86% (90%) for the three reference reactor designs. Correspondingly, this mitigates the penalties of inflexibility: forcing the core to operate at full capacity decreases the marginal value by just \$12/kW, \$67/kW, and \$150/kW, for the optimistic, mid-range, and pessimistic cores, respectively. See Fig. S5 for the value of dispatchable operation as a function of capacity penetration.

Figure 7 also shows the levelized cost of electricity (LCOE) for these plants. If the capital cost of a plant $\mathcal{C}_{\mathrm{plant}}$ and fixed charge rate f_{CR} are known as well as the variable cost $\pi^{VOM,total}$ and annual capacity factor f_{capacity}, one can compute

$$\mathrm{LCOE} = \frac{\mathcal{C}_{\mathrm{plant}} f_{\mathrm{CR}}}{8760\ f_{\mathrm{capacity}}} + \pi^{VOM,total}. \tag{1}$$

Here we take the capital cost of the plants to be equal to the marginal value at the given capacity penetration. As long as the plants are dispatchable, the maximum allowable LCOE *increases* with the variable cost, even as the maximum allowable capacity investment cost (Figure 4) falls. This effect is due to the distribution of electricity prices: plants make most of their revenues in relatively

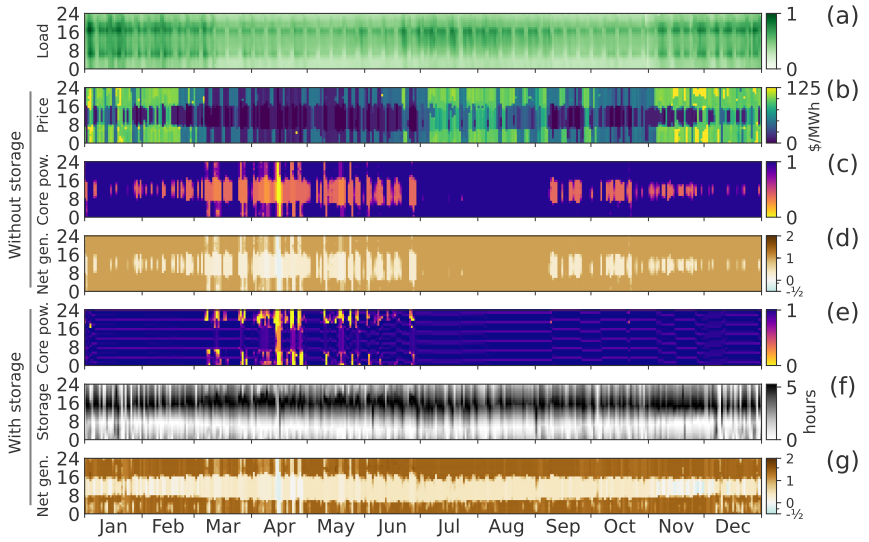

Figure 8: [Behavior of fusion plants throughout the year.] Optimal hourly operational behavior of the fusion cores and PCSs for plants with mid-range cores with and without a TSS option, in one typical zone of a medium market opportunity scenario with a total system fusion capacity of 50 GW. Part (a) shows the load in the zone, (b) shows the price, parts (c) and (e) shows thermal power output of the core normalized by its peak power, parts (d) and (g) show the net generation of the plant normalized by its long-run capacity, and part (f) shows the state of energy storage in the TSS measured in hours of the peak thermal capacity of the core. See also Figures S39 and S40 for operation of the other reference plants with and without thermal storage.

few hours of the year. It also shows that the equilibrium capacity penetration, and more generally, the merits of a plant for an electricity system, cannot be determined solely by the LCOE.

7. Annual and daily operation cycles

Figure 8 shows the operation of mid-range fusion plants in the medium market opportunity scenario with 50 GW of fusion capacity. Parts (c) and (e) show the operation of the cores and the normalized net output of the plants. In times such as the spring and fall where loads (a) and prices (b) are lower and solar power is available during the day, the plants follow a diurnal cycle, decreasing their output during the solar peak. During the periods of decreased output the plant is generally not shut off; rather, the power conversion system (PCS) is operated at levels approaching the minimum power level of 40%.

With a thermal storage system (TSS), the core runs during the solar peak, drawing electricity from the grid and storing heat while the PCS operates at its minimum capacity. In the evening, the oversized PCS draws power from the core and from storage, allowing plant to export power at 145% of its nominal (long-run) capacity.

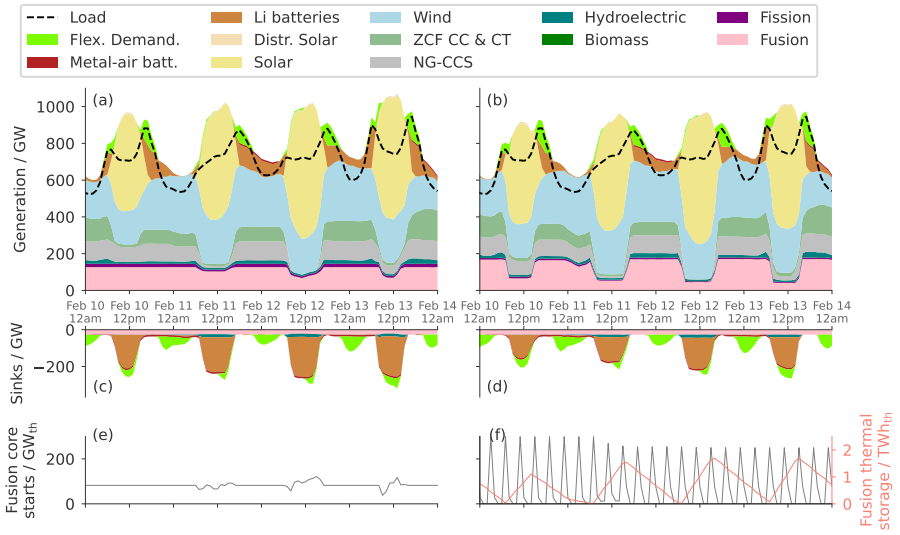

Figure 9: [Fusion plants interacting with other resources on an hourly timescale.] Operation of the whole electricity system during four days in February, for cases in the medium market opportunity scenario with 100 GW of mid-range fusion plants. At left, a case where the plants do not have a TSS; at right, a medium-cost thermal storage ($\$22/\mathrm{kW_{th}}$) can be built. Parts (a) and (b) show the generation by resources in the system, as well the nominal load; parts (c) and (d) show the sinks of power including energy storage and the fusion recirculating power, and parts (e) and (f) quantify the total thermal power of the fusion cores for which a pulse begins in each hour. Part (f) also shows the state of charge in the fusion thermal storage systems. In both cases, heat is produced by the cores at a constant rate, but with storage, the output of the plants are modulated daily by storing and discharging heat. Without the TSS, the fusion plants decrease their output when the variable renewables are sufficient. With the TSS, the fusion plants store their heat output during the day and release it at night.

The impact of a thermal storage system on operation can be seen further in Figure 9, which compares the behavior of plants with and without a TSS. Without a TSS, the pulses of the fusion fleet (shown in Part (e)) are staggered so that together they produce nearly constant power output (a), other than during daylight hours when their output is reduced. With a TSS, the precise timing of the pulses (shown in part (f)) is less important because the TSS buffers the PCS. Within the model, at least at this time, there is not a strong incentive to stagger the pulses. The TSS is filled and emptied on a diurnal cycle (part (f)) in order to generate power preferentially during the afternoon and night (part (b)). Incorporating a TSS with fusion also reduces the role of lithium battery storage. Less total battery capacity is required (Fig. S28) and as seen here, less charging and discharging takes place.

8. Regional opportunities for fusion

Fig 10 shows the most valuable places for 100 GW of fusion energy to be built (a) and produce energy (b) in the high market opportunity scenario. It is built preferentially in eastern and northern regions, likely due to the higher population density and lower resource potential of solar and wind there compared to regions further west. Compared to the equivalent case without fusion, it leads to fewer new transmission lines (c) needing to be constructed and (d) less energy generated from solar, NG-CCS and wind.

In the low and medium market opportunity scenarios, fusion is sited in similar regions. Less new transmission is required in these scenarios, and as the first 100 GW of fusion mostly substitute for new-build fission, the direct effect on transmission is limited; see also Figure S6.

9. Discussion

There are six major implications of this study. First, fusion could be a major firm resource for the US Eastern Interconnection, providing an annual net value of tens of billions of dollars, especially if renewables and storage, nuclear fission, or gas with carbon capture and storage fail to reach their cost targets. As an example, in the medium and high market opportunity scenarios, a plant with costs like that of ARIES-AT [38] (see Figure 4) would have equilibrium capacities of more than 100 GW, but zero in the low market opportunity scenario. In particular, fission is the primary competitor to fusion, so fusion stakeholders should closely monitor its development as well as trends in public acceptance of each. The United States may wish to consider fusion as a hedge for its energy portfolio [40] in case fission and other competitor resources fail to emerge. Alternately, it could develop the technology for export, especially for locations where land availability or safety concerns limit the viability of renewables and fission.

Second, the value of a fusion plant depends strongly on its marginal cost of net power generation (or variable operations and maintenance cost), so fusion

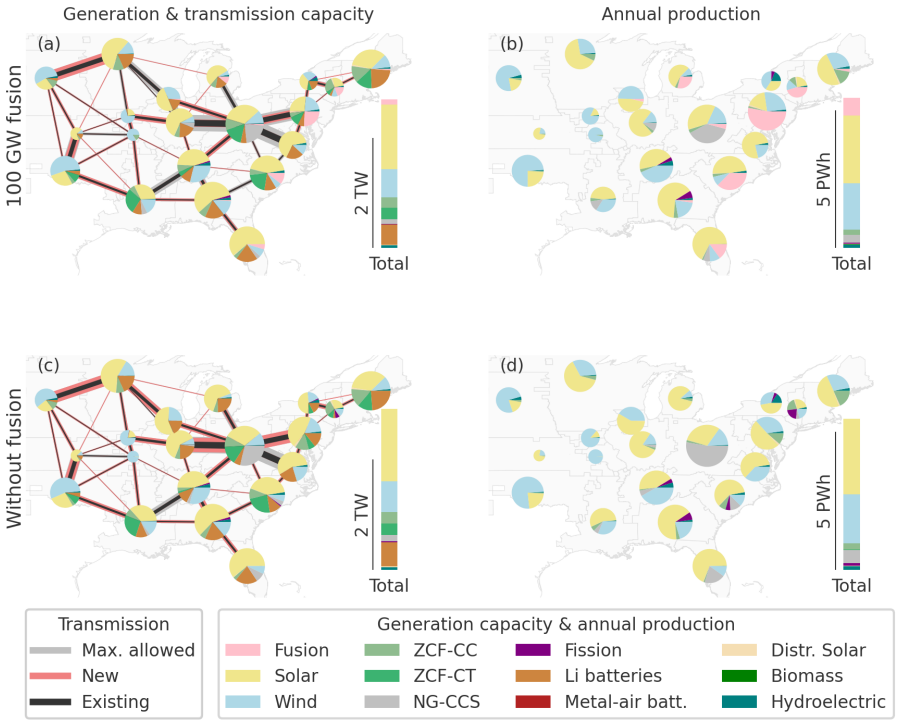

Figure 10: [Map of electricity resource deployment and production.] Generation capacity, transmission capacity, and annual production of each resource type in the high market opportunity scenario, for cases with 100 GW of mid-range fusion reactors (top) and without fusion (bottom). Fusion capacity is mostly along the eastern seaboard, where it is built (parts (a) versus (c)) instead of solar, wind, NG-CCS, and batteries and (parts (b) versus (d)) displaces a portion of their electricity production. The quantity of new transmission built (parts (a) versus (c)) is significantly smaller with the addition of fusion as a firm resource. See also Figures S35–S38 for maps of fusion deployment in other scenarios.

developers must take into account the costs of operating and maintaining future reactors, not only the capital cost. However, if fusion plants are dispatchable, then even a simple levelized cost of energy (LCOE) calculation which incorporates both fixed and variable costs does not capture all the complexities. For two plant designs with the same LCOE, the one with the higher variable cost (and lower capital and fixed costs) would reach a larger equilibrium capacity penetration. This suggests some changes to how plants should be designed, if one's goal is to maximize fusion capacity. If designs were optimized for LCOE in the past, then on the margin, more weight should be given to reducing capital costs at the expense of higher variable costs. This could mean using less durable components or subjecting components to higher loads, even if they must be replaced more often. This argument, along with the sustained periods of low prices in the models during spring and fall (Figure 8(b)), suggests that rather than the typical proposed maintenance cycles of, for example, four to six months followed by two years of operation[41], a plant with annual maintenance which is limited to the periods of low electricity prices could be an attractive option. While the model in this study neglects the needs for maintenance, a detailed assessment of the lost value due to these scheduled outages will be the subject of a future paper.

The above argument to trade capital costs for variable costs depends on fusion plants being dispatchable. The value attributable to dispatchable operation suggests that even fundamentally steady-state plants should either be designed with the ability to throttle their power output (once per day, on roughly half the days in the year, would be sufficient) or coupled to a more flexible power conversion system though a thermal storage system.

Third, plant value depends only weakly on the particulars of an hourly-scale pulse cycle when examined with an hourly resolution. If the technical challenges of pulsed tokamaks can be overcome, their varying output would not impose a significant penalty on their value, though future work should examine their integration with the grid on finer spatial and temporal scales[42].

Fourth, while not studied explicitly, the strong dependence of plant value on variable cost suggests that multiple classes of fusion plants at different locations on the capital–variable cost frontier could coexist.

Fifth, our study finds that the equilibrium capacity penetration of fusion increases significantly with relatively small decreases in the cost of a marginal plant. This suggests that if cost targets for an initial market penetration can be met, further cost decreases driven by incremental improvements and learning-by-doing could allow fusion to reach a much higher capacity.

Finally, integrated thermal storage such as molten salt increases the plant value by a modest amount by better serving daily demand cycles. It would be especially valuable while the total fusion capacity is small, and would further be valuable if early plants need to operate in a quasi-steady-state mode (for example due to a limited tolerance for thermal cycling). For an initial market penetration, as long as the power conversion system remains dispatchable, the core need not be.

This study has several limitations due to the nature of the GenX capacity

expansion model and our method of using it. First, our study cannot address the question of the optimum unit size for fusion plants as all costs are assumed to scale linearly with capacity. While magnetic fusion concepts like tokamaks and stellarators tend to multi-gigawatt scales when optimizing for the minimum cost-per-watt, the procuring utilities have finite ability to finance project costs, and maximum scales may be limited by concerns about the stability of the grid[43] should a plant suffer an unplanned outage. However, the question of the optimum unit size is distinct from the cost thresholds we have determined. For our study of plants with thermal storage systems, economies of scale would affect the optimal capacity ratios for the core, power conversion system, and storage.

Second, the temporal and spatial resolution of the simulations are likely somewhat favorable to fusion. The hourly time basis used here does not resolve the details of a tokamak pulse cycle. Future work could use finer steps to resolve any start-up power flows from the grid, which could lead to price spikes. Similarly, the coarse spatial resolution underestimates the challenges of integrating pulsed reactors with the grid[34].

Third, GenX optimizes capacity expansion for a long-run equilibrium, but the energy transition is dynamic. The two modeled capacity expansion cycles, which represent 15 yr, each use a single representative year with perfect foresight and rational decision-making. We ignore cost-decreasing learning effects, which could lead to "technology lock-in" if, for example, small modular fission reactors are successfully mass-produced and adopted. We implicitly assume that fusion becomes available just as electricity demand grows, as opposed to adoption being driven by retirements from the existing fleet[44], and ignore limitations to fusion's growth rate due to finite tritium stocks[45].

Fourth, in our studies, the electricity system is not coupled with wider energy markets, and fuel costs are both fixed throughout the year and independent of demand. Conversely, applications of fusion energy other than electricity generation, such as co-production of industrial heat or hydrogen, could add value to fusion plants, but these opportunities are not studied. Neither is the use of fusion to re-power existing thermal plants[8], which could reduce capital costs and make fusion easier to site.

Finally, we assume perfect availability for fusion with no unscheduled downtime and no need for scheduled maintenance periods. The latter is a planned topic of study.

10. Experimental Procedures

Resource availability

Lead contact

Further information and requests for resources and materials should be directed to and will be fulfilled by the lead contact, Jacob A. Schwartz (`jacobas@princeton.edu`).

Materials availability

This study did not generate new unique materials.

Data and code availability

Data for this paper, as well as the code used for analyses, are archived at the Princeton Dataspace[46]. A branch of GenX v0.2.0[47] was used for the model runs. GenX is available at `https://github.com/GenXProject/GenX`.

10.1. Modeling technique

We studied the value of fusion plants of various designs in a United States Eastern Interconnect electricity system with net-zero CO_2 emissions during a period representing 2036–2050. While this period is somewhat early for a significant build-out of commercial fusion plants, it was chosen as a compromise due to the increasing uncertainty associated with periods further into the future.

We used the GenX capacity expansion and operations code[13]. Given a representation of the electricity system, described as a set of geographic zones, transmission networks between zones, hourly loads, hourly availability profiles for variable renewable resources and time-shiftable loads, sets of existing resources, and resources which could be built, it determines the sets of resources to be built or retired and the hourly operation of each resource in order to minimize the annual cost of the electricity system. The model contains 20 geographic zones, each describing one or more of the regions based on the EPA Integrated Planning Model (IPM `v6`) regions[48] in the Eastern Interconnection. A full year (8760 h) of hourly operation is modeled.

We examined three main scenarios with differing costs of resources other than fusion; we refer to these as the low, medium, and high fusion market opportunity scenarios. Each scenario has the same load profiles, but different quantities of time-shiftable loads. Input data are from a variety of sources, including PUDL[49] and the NREL Annual Technology Baseline (ATB) 2021[50]. Eleven variant scenarios are also described in the SI.

For each of the three main scenarios, in order to determine the resources existing at the start of the 2036–2050 period, we performed a simulation representing the years 2021–2035, without the net-zero CO_2 constraint; the generator capacity expansion results were used as inputs for the subsequent model runs.

10.2. Resource cost and operational assumptions

Table 2 lists the capital costs of the resources which can be built in the 2036–2050 simulations. Capital costs, fixed operational costs, variable operational costs, and heat rates for new-build technologies in the medium and high market opportunity scenarios generally follow the 'Moderate' cost assumptions from the ATB, while the low market opportunity scenario generally follows the 'Advanced' cost assumptions. Capital costs are taken to be the average of those in the period 2036–2050.

Exceptions are metal-air batteries, which are not listed in the ATB and for which we use cost and performance assumptions from[51], and NG-CCS plants.

Table 2: Median capital costs of generation and storage in $/kW and $/kWh in 2036–2050 for the three market scenarios, the real weighted average cost of capital (WACC) in % for each technology, and the assumed lifetime in years. Low-cost fission is used only in the so-named variant scenarios.

	Low	Medium	High	Real WACC	Lifetime
Utility-scale Solar PV	536	686	686	2.57	30
Onshore wind	586	826	826	3.00	30
Offshore wind	1603	1918	1918	3.21	30
ZCF-CT	787	787	787	3.34	30
ZCF-CC	942	942	942	3.34	30
NG-CCS	2318	2318	2318	3.34	30
Fission	4176	6233	9348	3.34	40
Fission (low-cost)	3740	4986	6233	3.34	40
Li batteries - power	80	187	187	2.57	15
Li batteries - storage	86	117	117	2.57	15
Metal-air batteries - power	800	1200	2000	2.57	25
Metal-air batteries - storage	8	12	20	2.57	25

Because only the 'Conservative' cost and performance assumptions for NG-CCS in the ATB assume a conventional combined cycle plant (rather than a fuel cell or an interpolation between the two), we use the conservative case as our baseline for this category of plant. NG-CCS cost and performance parameters are adjusted further to reflect the requirement of 100% carbon capture efficiency in our system, an increase from the 90% efficiency assumed in the ATB: capital cost is increased by $116/kW, heat rate by 0.365, fixed OM by $9.67/(kW yr), and variable OM by 7.6%. We further consider the need for CO_2 transport and storage infrastructure, the cost of which varies by model zone. CO_2 pipeline construction costs are added to NG-CCS plant investment costs, and are calculated using methodology developed in[52], assuming an average plant size of 500 MW, a 100% utilization rate, and a length equal to the distance between the largest major metro area in each GenX zone and the edge of the nearest CO_2 injection basin. Variable injection costs per ton of CO_2 are added to NG-CCS plant variable operational costs, and vary by injection basin. CO_2 pipeline costs by GenX zone are listed in Table S3.

Costs for the ZCF combustion turbine (CT) and closed cycle gas turbine (CC) correspond to those of the "Natural Gas FE CT" and "Natural Gas FE CC", respectively. Capital costs of these combustion plants do not vary by scenario, but the fuel costs do; see Table 3.

Fission costs in the medium fusion opportunity scenario are from the "moderate" ATB scenario, which are from the EIA Annual Energy Outlook 2021[53]. The low and high market opportunity scenarios use ⅔ and ³⁄₂ of this cost, respectively, and the three low-cost nuclear scenarios use ³⁄₅, ⁴⁄₅, and ⁵⁄₅ of this

Table 3: Fuel costs and total variable costs in $/MMBTU and $/MWh, respectively, in 2036–2050, for the three market opportunity scenario classes.

	Low		Medium		High	
ZCF-CT	10.81	110.01	14.41	145.00	19.21	191.66
ZCF-CC	10.81	70.49	14.41	93.39	19.21	123.92
NG-CCS	2.75	33.20	3.75	40.72	6.50	61.39
Fission	0.73	9.96	0.73	9.96	0.73	9.96
Li batteries		0.15		0.15		0.15
Metal-air storage		0		0		0
Fusion: PCS operation		1.74		1.74		1.74

cost, respectively.

Lithium ion batteries have charge and discharge efficiencies of 0.92 each and metal-air storage has charge and discharge efficiencies of 0.65 each, for round-trip efficiencies of 0.85 and 0.42, respectively.

Resources have an additional cost to account for transmission spur lines, with regional costs from $3686 per MW-mile to $6320 per MW-mile. The length of the spur lines is shown in Table S4; wind and solar have variable spur line lengths and costs from a method developed for the Net-Zero America study [52].

Table 3 lists the fuel costs and total variable costs of the resources in the 2036–2050 cases in the fusion market opportunity scenario classes. The total variable cost includes the cost of the fuel and the variable OM cost of the plant itself. The two ZCF fuel resources nominally use the same type of fuel, but the ZCF-CC plant is more efficient, so its total variable cost is lower. For fusion we list the variable OM cost of the power conversion system (PCS) only. This cost is incurred proportional to the gross generation, so for a fusion plant with 50% recirculating power the PCS variable OM cost would be twice as high per *net* MWh_e. The fusion plant also has a VOM cost for the core operation, but these vary by the reactor design: see Table 1 of the main paper.

Zonal costs for conventional fuel types are from the EIA Annual Energy Outlook [53]. Natural gas costs for the Low, Medium, and High market opportunity cases are taken from the AEO's high oil and gas supply, reference, and low oil and gas supply cases, respectively. The nature of the zero-carbon fuel is not explicit, but the cost of ZCF in the Medium market opportunity scenario is set equal to the average H_2 cost in the three high-electrification scenarios in the Net-Zero America report [52], $15.20/GJ. ZCF costs in the Low and High market opportunity cases are ⅔ and ³⁄₂ of this value, respectively.

Power flow between resources and loads inside zones is considered to be lossless; this is sometimes called the copper-plate assumption. Power flow between zones is limited by the inter-regional transmission capacity. These start at 2020 values. The capacity of each route can be expanded by up to 150% or 1.5 GW, whichever is larger. This assumption is somewhat arbitrary, but even either forbidding new transmission or allowing unlimited transmission does not affect the value of fusion by more than $150/kW in the medium market opportunity

scenario or more than 900/kW in the high market opportunity scenario; see Figure S6. Costs per GW-mile for transmission are dependent on the regions connected. The existing transmission capacity and maximum possible capacities are listed in Table S6. Transmission losses are linear with the power transmitted between zones.

10.3. Pulsed tokamak plant model

When assessing costs, such as the value of the core (as in Figure 6), the core represents not just the fusion chamber itself, but all parts of the plant other than the TSS and PCS. The structure of the implementation motivates the component definitions. The core represents most of the plant: the reactor itself, maintenance facilities, land, parking lots, waste storage, and so on. The model PCS includes some heat exchangers, the turbines, generators, and heat rejection systems. Its costs are assumed to scale linearly with its rated power capacity. Any heat exchangers upstream of the TSS are part of the core. The model TSS includes tanks required for inter-hourly energy storage, but does not include additional piping, heat exchangers, or other systems which affect the input or output power capacity of the storage system; those are part of the core. The TSS costs scale linearly with the energy storage capacity. The core also includes any intra-hourly energy storage systems which are required for interfacing with the PCS.

In a real reactor, certain components may need to be replaced due to cyclic fatigue rather than damage from cumulative neutron exposure; this could be modeled by adding a finite cost to start a pulse, but it is not implemented here. In this study the fusion plant is operated at its maximum cadence throughout most of the year, so pricing the pulse start in addition to the heat generated would lead to little difference in operation.

Reference reactors

The pessimistic core loosely models a plant similar to DEMO (which is not a competitive commercial power plant[31,54]). The two-hour total cycle time is a rounding down of the ~ 8000 s total cycle time including a 2 h flat-top, and the 0.15 h dwell time is a rounding down of the < 10 minute length, both listed in Table 3 of the overview paper by Federici et al[31]. The active and recirculating power fractions are both set to 0.2. Together these represent an improvement on the 475 MW and 392 MW of *total* recirculating power demands required by the steady state electrical systems during the burn flat-top and dwell period, respectively, as estimated as the "active power" for the HCPB design (Figure 15 and Table 6) by Gaio et al[42]. Note that here "active" is in contrast to reactive power. For the "indirect" coupling configuration between the fusion core and PCS, the gross electric power is 900 MW, so this would translate to a $r_{\text{pass}} = 0.435$ and $r_{\text{act}} = 0.092$. In our model moving a fixed quantity from r_{pass} to r_{act} is always beneficial, so $r_{\text{act}} = r_{\text{pass}} = 0.2$ is strictly an improvement. The start power and start energy fractions are roughly estimated from the size of the loads of the DEMO pulsed power electrical network (PPEN)[34]. The variable

operations and maintenance cost is estimated by applying the Sheffield costing method[9] to a 2015 version of DEMO[55] and computing the costs of blanket and divertor replacement; this came to \$7.3/$\mathrm{MWh_{th}}$ and was rounded down to \$5/$\mathrm{MWh_{th}}$.

The mid-range core is based off the pessimistic core, but with a pulse cycle duration of 4 h and with recirculating power parameters half as large as those of the pessimistic core. Its $\pi^{VOM,th}$ is the average of those of the two other cores.

The optimistic core is based on an optimistic view of the ARC reactor[15,33]. The 2020 ARC design point[33] describes it as having roughly 30 minute pulses; this is changed to 1 h in order to fit in our hour-based model; the dwell time was increased proportionally. It has a total recirculating power of 4.3%[33], no external start power, and a variable operations and maintenance cost arbitrarily set at 1/5th that of the pessimistic core. Though this model must start a pulse every hour, because there is zero start energy and start power this is not a significant burden; we call it "optimistic" due to its low total VOM cost.

Table 1 lists parameters for the fusion plant which can be derived from the core and power conversion system parameters, assuming that the plant is operated at its maximum capacity. The core active fraction

$$f_{\mathrm{act}} = \left(1 - \frac{t_{\mathrm{dw}}}{t_{\mathrm{pu}}}\right). \tag{2}$$

is the fraction of the time that the core is producing heat, and when the active recirculating power is required. The core net capacity factor

$$f_{\mathrm{netavgcap}} = f_{\mathrm{act}}\left(1 - r_{\mathrm{act}}\right) - r_{\mathrm{pass}} - \frac{e_{\mathrm{start}}}{t_{\mathrm{pu}}}. \tag{3}$$

is the ratio of the time-averaged net electric power produced to the gross electric power generation capacity. The core peak thermal capacity $\mathrm{CAP}^{\mathrm{th}}_{\mathrm{peak}}$ is related to the plant time-average net electrical capacity $\overline{\mathrm{CAP}}^{\mathrm{el}}_{\mathrm{net}}$,

$$\overline{\mathrm{CAP}}^{\mathrm{el}}_{\mathrm{net}} = \eta^{discharge} f_{\mathrm{netavgcap}} \mathrm{CAP}^{\mathrm{th}}_{\mathrm{peak}}. \tag{4}$$

In this paper, the fusion plant capacity penetration is specified in terms of $\overline{\mathrm{CAP}}^{\mathrm{el}}_{\mathrm{net}}$. This allows a comparison between cores with different operational characteristics. The marginal cost of net generation

$$\pi^{VOM,total} = \frac{f_{\mathrm{act}}\left(\pi^{VOM,th} + \eta^{discharge}\pi^{VOM}\right)}{\eta^{discharge} f_{\mathrm{netavgcap}}} \tag{5}$$

reflects the variable operations and maintenance cost for the core and generator, taking into account the recirculating power and dwell times. As shown in Figure 3, for plants without a thermal storage system, the required total plant cost is largely determined by this quantity. Finally, the recirculating power fraction

$$f_{\mathrm{recirc}} = \frac{f_{\mathrm{act}} r_{\mathrm{act}} + r_{\mathrm{pass}} + e_{\mathrm{start}}/t_{\mathrm{pu}}}{f_{\mathrm{act}}}. \tag{6}$$

is the fraction of the gross power generated which must be used to operate the device itself. This can be related to the plant's time-averaged engineering gain Q_{eng}[56]:

$$Q_{\text{eng}} = (1 - f_{\text{recirc}})/f_{\text{recirc}}. \tag{7}$$

10.4. Plant cost threshold determinations

In this paper we determine the relationship between the cost of fusion and its equilibrium capacity penetration in the electricity system. While perhaps the most straightforward method would be to find the capacity penetration as a function of cost, here we find the cost as a function of the capacity penetration. The method employed is not entirely straightforward, but has some advantages in practice, and ultimately achieves the same results.

The most obvious method would have been to set a trial cost for the fusion core and solve the capacity expansion problem to determine the total fusion capacity in the optimized electricity system. While this method is conceptually straightforward, it has a minor disadvantage: if the cost of fusion core was too high, no fusion plants would be built, wasting a several-hour computation. Additionally, finding the cost threshold for an initial penetration into the market—a key metric for fusion commercialization—becomes a root-finding problem.

Instead we use a method[5–7] that determines the marginal value of a plant as a function of its capacity penetration. Unless the user requests an extremely large fusion capacity penetration (beyond 350 GW in the scenarios described here), this method always results in a nonzero marginal value for fusion energy. It is thus arguably more efficient in its use of compute time. There are two additional advantages. First, differences in the operational parameters of the plant (such as those explored in Fig. 3) directly translate into differences in value, rather than differences in the equilibrium capacity penetration. We believe this to be a more relevant metric for fusion developers and policymakers. Second, the value-based approach perhaps has a conceptual advantage, in that it disentangles the question of the cost of a plant from the notion of its value to the system as a whole. The method is explained below.

The plant is composed of the core, PCS, and TSS. In each case, the investment cost and fixed operations and maintenance costs of the fusion core are set to zero, and the total net fusion capacity in the system is fixed by a constraint. The value of the fusion core is calculated as the *dual value* of this constraint: the amount by which the model's objective function would decrease given a relaxation of the constraint by one unit. Because system costs would decline by this amount were an additional unit of fusion core capacity deployed in the system, this can equivalently be interpreted as the minimum cost that the fusion core could have for this deployment to be profitable. For equilibrium market conditions in GenX the profit of a marginal plant is exactly zero, and so we can interpret the core value at a specified total fusion penetration as the exact core *cost* at which fusion would naturally achieve that penetration in a competitive market. For plants without a TSS the ratio of fusion core capacity to PCS capacity is fixed. The sum of the (known) annual PCS cost and the core

value is the maximum annual cost of the whole fusion plant, which includes the annualized investment cost and the fixed operations and maintenance costs. We refer to this as the plant value, or equivalently, the threshold cost for a marginal plant. In cases where a TSS is allowed, a precise equivalent to this quantity cannot be determined by simply adding its costs, since the ratios of PCS and TSS capacities to fusion core capacities vary strongly as a function of the fusion capacity penetration. Instead we refer solely to the value of the core itself.

As a check of this system value method we performed a run (using the "straightforward" method) with the cost of the fusion core set equal to the marginal value previously determined at 100 GW of capacity penetration. The optimal fusion capacity was 99.77 GW. The imperfection is due to finite tolerances in the optimizer.

Supplemental information description

The supplemental information (SI) describes the model configuration, economic parameters, and other input data for the main scenarios, and for eleven variant scenarios not discussed in the main text. It contains a formal description of the fusion plant implementation and a full set of input parameters. The SI also includes additional outputs: plots of added value and relative component sizes of fusion plants with thermal storage, capacity and energy production mixes for the various scenarios, maps showing where fusion plants are built, and charts showing the operational behaviors of the other reference plants.

Acknowledgments

Thanks to Greg Schively for help with PowerGenome.

J. A. Schwartz and E. Kolemen were supported through the U.S. Department of Energy under contract number DE-AC02-09CH11466. The United States Government retains a non-exclusive, paid-up, irrevocable, world-wide license to publish or reproduce the published form of this manuscript, or allow others to do so, for United States Government purposes.

W. Ricks received support for this work from the Princeton Zero-Carbon Technology Consortium, which is supported by unrestricted gifts from General Electric, Google, and ClearPath.

Author contributions

JAS: Conceptualization, Methodology, Software, Formal analysis, Investigation, Data curation, Writing, Visualization. WR: Methodology, Software, Resources, Writing-original draft. EK: Conceptualization, Methodology, Writing-review and editing, Supervision, Funding acquisition. JJ: Conceptualization, Methodology, Software, Writing-review and editing, Supervision, Funding acquisition.

Declaration of Interests

J. D. J. is a consultant to Clean Air Task Force, an Advisory Board Member for Eavor Technologies and Rondo Energy, a technical advisor to Energy Impact Partners and MUUS Climate Partners, and an owner and partner with DeSolve LLC, which has provided consulting services within the past 12 months to JPMorgan Chase and Rice Acquisition Corp 2.

References

[1] C. Windsor, Can the development of fusion energy be accelerated? An introduction to the proceedings, Philosophical Transactions of the Royal Society A: Mathematical, Physical and Engineering Sciences 377 (2141) (2019) 20170446. doi:10.1098/rsta.2017.0446.

[2] T. Okazaki, Fusion Reactor Design: Plasma Physics, Fuel Cycle System, Operation and Maintenance, Wiley-VCH, Berlin, 2021. doi:10.1002/9783527832934.

[3] G. H. Miley, Review of Direct Conversion of Nuclear Energy, Fusion Technology 20 (4P2) (1991) 977–986. doi:10.13182/FST91-A11946970.

[4] N. A. Sepulveda, J. D. Jenkins, F. J. de Sisternes, R. K. Lester, The Role of Firm Low-Carbon Electricity Resources in Deep Decarbonization of Power Generation, Joule 2 (11) (2018) 2403–2420. doi:10.1016/j.joule.2018.08.006.

[5] F. J. de Sisternes, J. D. Jenkins, A. Botterud, The value of energy storage in decarbonizing the electricity sector, Applied Energy 175 (2016) 368–379. doi:10.1016/j.apenergy.2016.05.014.

[6] D. S. Mallapragada, N. A. Sepulveda, J. D. Jenkins, Long-run system value of battery energy storage in future grids with increasing wind and solar generation, Applied Energy 275 (2020) 115390. doi:10.1016/j.apenergy.2020.115390.

[7] C. F. Heuberger, I. Staffell, N. Shah, N. M. Dowell, A systems approach to quantifying the value of power generation and energy storage technologies in future electricity networks, Computers & Chemical Engineering 107 (2017) 247–256. doi:10.1016/j.compchemeng.2017.05.012.

[8] M. C. Handley, D. Slesinski, S. C. Hsu, Potential Early Markets for Fusion Energy, J Fusion Energ 40 (2) (2021) 18. arXiv:2101.09150, doi:10.1007/s10894-021-00306-4.

[9] J. Sheffield, S. L. Milora, Generic Magnetic Fusion Reactor Revisited, Fusion Science and Technology 70 (1) (2016) 14–35. doi:10.13182/FST15-157.

[10] L. M. Waganer, ARIES Cost Account Documentation, Tech. Rep. UCSD-CER-13-01, Center for Energy Research, University of California, San Diego, San Diego, CA (Jun. 2013).

[11] G. R. Tynan, A. Abdulla, How might controlled fusion fit into the emerging low-carbon energy system of the mid-twenty-first century?, Philosophical Transactions of the Royal Society A: Mathematical, Physical and Engineering Sciences 378 (2184) (2020) 20200009. doi:10.1098/rsta.2020.0009.

[12] I. M. Müller, M. Reich, F. Warmer, H. Zohm, T. Hamacher, S. Günter, Analysis of technical and economic parameters of fusion power plants in future power systems, Fusion Engineering and Design 146 (2019) 1820–1823. doi:10.1016/j.fusengdes.2019.03.043.

[13] MIT Energy Initiative and Princeton University ZERO lab, GenX: A configurable power system capacity expansion model for studying low-carbon energy futures (Mar. 2022).

[14] F. N. Al Farsi, M. H. Albadi, N. Hosseinzadeh, A. H. Al Badi, Economic Dispatch in power systems, in: 2015 IEEE 8th GCC Conference & Exhibition, IEEE, Muscat, Oman, 2015, pp. 1–6. doi:10.1109/IEEEGCC.2015.7060068.

[15] B. Sorbom, J. Ball, T. Palmer, F. Mangiarotti, J. Sierchio, P. Bonoli, C. Kasten, D. Sutherland, H. Barnard, C. Haakonsen, J. Goh, C. Sung, D. Whyte, ARC: A compact, high-field, fusion nuclear science facility and demonstration power plant with demountable magnets, Fusion Engineering and Design 100 (2015) 378–405. doi:10.1016/j.fusengdes.2015.07.008.

[16] A. J. Creely, M. J. Greenwald, S. B. Ballinger, D. Brunner, J. Canik, J. Doody, T. Fülöp, D. T. Garnier, R. Granetz, T. K. Gray, C. Holland, N. T. Howard, J. W. Hughes, J. H. Irby, V. A. Izzo, G. J. Kramer, A. Q. Kuang, B. LaBombard, Y. Lin, B. Lipschultz, N. C. Logan, J. D. Lore, E. S. Marmar, K. Montes, R. T. Mumgaard, C. Paz-Soldan, C. Rea, M. L. Reinke, P. Rodriguez-Fernandez, K. Särkimäki, F. Sciortino, S. D. Scott, A. Snicker, P. B. Snyder, B. N. Sorbom, R. Sweeney, R. A. Tinguely, E. A. Tolman, M. Umansky, O. Vallhagen, J. Varje, D. G. Whyte, J. C. Wright, S. J. Wukitch, J. Zhu, the SPARC Team, Overview of the SPARC tokamak, Journal of Plasma Physics 86 (5) (Oct. 2020). doi:10.1017/S0022377820001257.

[17] M. Gryaznevich, V. A. Chuyanov, Y. Takase, Pulsed Spherical Tokamak—A New Approach to Fusion Reactors, Plasma 5 (2) (2022) 247–257. doi:10.3390/plasma5020019.

[18] R. J. Buttery, J. M. Park, J. McClenaghan, D. B. Weisberg, J. M. Canik, J. R. Ferron, A. M. Garofalo, C. T. Holcomb, J. A. Leuer, P. B. Snyder, The advanced tokamak path to a compact net electric fusion pilot plant, Nucl. Fusion 61 (4) (2021) 046028. doi:10.1088/1741-4326/abe4af.

[19] F. Najmabadi, A. R. Raffray, S. I. Abdel-Khalik, L. Bromberg, L. Crosatti, L. El-Guebaly, P. R. Garabedian, A. A. Grossman, D. Henderson, A. Ibrahim, T. Ihli, T. B. Kaiser, B. Kiedrowski, L. P. Ku, J. F. Lyon, R. Maingi, S. Malang, C. Martin, T. K. Mau, B. Merrill, R. L. Moore, R. J. Peipert, D. A. Petti, D. L. Sadowski, M. Sawan, J. H. Schultz, R. Slaybaugh, K. T. Slattery, G. Sviatoslavsky, A. Turnbull, L. M. Waganer, X. R. Wang, J. B. Weathers, P. Wilson, J. C. Waldrop, M. Yoda, M. Zarnstorffh, The ARIES-CS Compact Stellarator Fusion Power Plant, Fusion Science and Technology 54 (3) (2008) 655–672. doi:10.13182/FST54-655.

[20] F. Warmer, V. Bykov, M. Drevlak, A. Häußler, U. Fischer, T. Stange, C. Beidler, R. Wolf, From W7-X to a HELIAS fusion power plant: On engineering considerations for next-step stellarator devices, Fusion Engineering and Design 123 (2017) 47–53. doi:10.1016/j.fusengdes.2017.05.034.

[21] J. Alonso, I. Calvo, D. Carralero, J. Velasco, J. García-Regaña, I. Palermo, D. Rapisarda, Physics design point of high-field stellarator reactors, Nucl. Fusion 62 (3) (2022) 036024. doi:10.1088/1741-4326/ac49ac.

[22] M. Dunne, E. I. Moses, P. Amendt, T. Anklam, A. Bayramian, E. Bliss, B. Debs, R. Deri, T. D. de la Rubia, B. El-Dasher, J. C. Farmer, D. Flowers, K. J. Kramer, L. Lagin, J. F. Latkowski, J. Lindl, W. Meier, R. Miles, G. A. Moses, S. Reyes, V. Roberts, R. Sawicki, M. Spaeth, E. Storm, Timely Delivery of Laser Inertial Fusion Energy (LIFE), Fusion Science and Technology 60 (1) (2011) 19–27. doi:10.13182/FST10-316.

[23] V. T. Tikhonchuk, Progress and opportunities for inertial fusion energy in Europe, Phil. Trans. R. Soc. A. 378 (2184) (2020) 20200013. doi:10.1098/rsta.2020.0013.

[24] M. Laberge, Magnetized Target Fusion with a Spherical Tokamak, J Fusion Energ 38 (1) (2019) 199–203. doi:10.1007/s10894-018-0180-3.

[25] M. Laberge, Magnetized Target Fusion at General Fusion (2021).

[26] T. Fowler, R. Moir, T. Simonen, A new simpler way to obtain high fusion power gain in tandem mirrors, Nucl. Fusion 57 (5) (2017) 056014. doi:10.1088/1741-4326/aa5e54.

[27] N. Rostoker, M. W. Binderbauer, H. J. Monkhorst, Colliding Beam Fusion Reactor, Science 278 (5342) (1997) 1419–1422. doi:10.1126/science.278.5342.1419.

[28] W. Meier, R. Schmitt, R. Abbott, J. Latkowski, S. Reyes, Nuclear design considerations for Z-IFE chambers, Fusion Engineering and Design 81 (8-14) (2006) 1661–1666. doi:10.1016/j.fusengdes.2005.08.092.

[29] U. Shumlak, Z-pinch fusion, Journal of Applied Physics 127 (20) (2020) 200901. doi:10.1063/5.0004228.

[30] M. Shimada, D. Campbell, V. Mukhovatov, M. Fujiwara, N. Kirneva, K. Lackner, M. Nagami, V. Pustovitov, N. Uckan, J. Wesley, N. Asakura, A. Costley, A. Donné, E. Doyle, A. Fasoli, C. Gormezano, Y. Gribov, O. Gruber, T. Hender, W. Houlberg, S. Ide, Y. Kamada, A. Leonard, B. Lipschultz, A. Loarte, K. Miyamoto, V. Mukhovatov, T. Osborne, A. Polevoi, A. Sips, Progress in the ITER Physics Basis, Chapter 1: Overview and summary, Nuclear Fusion 47 (6) (2007) S1. doi:10.1088/0029-5515/47/6/S01.

[31] G. Federici, C. Bachmann, L. Barucca, W. Biel, L. Boccaccini, R. Brown, C. Bustreo, S. Ciattaglia, F. Cismondi, M. Coleman, V. Corato, C. Day, E. Diegele, U. Fischer, T. Franke, C. Gliss, A. Ibarra, R. Kembleton, A. Loving, F. Maviglia, B. Meszaros, G. Pintsuk, N. Taylor, M. Tran, C. Vorpahl, R. Wenninger, J. You, DEMO design activity in Europe: Progress and updates, Fusion Engineering and Design 136 (2018) 729–741. doi:10.1016/j.fusengdes.2018.04.001.

[32] P. Libeyre, N. Mitchell, D. Bessette, Y. Gribov, C. Jong, C. Lyraud, Detailed design of the ITER central solenoid, Fusion Engineering and Design 84 (7-11) (2009) 1188–1191. doi:10.1016/j.fusengdes.2009.01.090.

[33] B. Sorbom, A. Creely, C. Tse, Recent developments in the design of ARC (Oct. 2020).

[34] S. Minucci, S. Panella, S. Ciattaglia, M. C. Falvo, A. Lampasi, Electrical Loads and Power Systems for the DEMO Nuclear Fusion Project, Energies 13 (9) (2020) 2269. doi:10.3390/en13092269.

[35] H. Zohm, On the Minimum Size of DEMO, Fusion Science and Technology 58 (2) (2010) 613–624. doi:10.13182/FST10-06.

[36] N. Blair, N. DiOrio, J. Freeman, P. Gilman, S. Janzou, T. Neises, M. Wagner, System Advisor Model (SAM) General Description, Tech. Rep. NREL/TP-6A20-70414, National Renewable Energy Laboratory (May 2018).

[37] C. S. Turchi, M. Boyd, D. Kesseli, P. Kurup, M. S. Mehos, T. W. Neises, P. Sharan, M. J. Wagner, T. Wendelin, CSP Systems Analysis - Final Project Report, Tech. Rep. NREL/TP–5500-72856, 1513197, National Renewable Energy Laboratory (May 2019). doi:10.2172/1513197.

[38] F. Najmabadi, A. Abdou, L. Bromberg, T. Brown, V. Chan, M. Chu, F. Dahlgren, L. El-Guebaly, P. Heitzenroeder, D. Henderson, H. St. John, C. Kessel, L. Lao, G. Longhurst, S. Malang, T. Mau, B. Merrill, R. Miller, E. Mogahed, R. Moore, T. Petrie, D. Petti, P. Politzer, A. Raffray, D. Steiner, I. Sviatoslavsky, P. Synder, G. Syaebler, A. Turnbull, M. Tillack, L. Waganer, X. Wang, P. West, P. Wilson, The ARIES-AT advanced tokamak, Advanced technology fusion power plant, Fusion Engineering and Design 80 (1-4) (2006) 3–23. doi:10.1016/j.fusengdes.2005.11.003.

[39] L. Barucca, E. Bubelis, S. Ciattaglia, A. D'Alessandro, A. Del Nevo, F. Giannetti, W. Hering, P. Lorusso, E. Martelli, I. Moscato, A. Quartararo, A. Tarallo, E. Vallone, Pre-conceptual design of EU DEMO balance of plant systems: Objectives and challenges, Fusion Engineering and Design 169 (2021) 112504. doi:10.1016/j.fusengdes.2021.112504.

[40] United States of America, The long-term strategy of the United States: Pathways to net-zero greenhouse gas emissions by 2050 (Nov. 2021).

[41] O. Crofts, J. Harman, Maintenance duration estimate for a DEMO fusion power plant, based on the EFDA WP12 pre-conceptual studies, Fusion Engineering and Design 89 (9-10) (2014) 2383–2387. doi:10.1016/j.fusengdes.2014.01.038.

[42] E. Gaio, A. Ferro, A. Lampasi, A. Maistrello, M. Dan, M. Falvo, F. Gasparini, F. Lunardon, A. Magnanimo, M. Manganelli, S. Minucci, S. Panella, M. Proietti Cosimi, D. Ratti, L. Barucca, S. Ciattaglia, T. Franke, G. Federici, R. Piovan, Status and challenges for the concept design development of the EU DEMO Plant Electrical System, Fusion Engineering and Design 177 (2022) 113052. doi:10.1016/j.fusengdes.2022.113052.

[43] S. Takeda, S. Konishi, Y. Yamamoto, R. Kasada, S. Sakurai, Dynamic Simulation-Based Case Study of Fusion on Small-Scale Electrical Grids, Fusion Science and Technology 68 (2) (2015) 341–345. doi:10.13182/FST15-106.

[44] L. Spangher, J. S. Vitter, R. Umstattd, Characterizing fusion market entry via an agent-based power plant fleet model, Energy Strategy Reviews 26 (2019) 100404. doi:10.1016/j.esr.2019.100404.

[45] R. J. Pearson, A. B. Antoniazzi, W. J. Nuttall, Tritium supply and use: A key issue for the development of nuclear fusion energy, Fusion Engineering and Design 136 (2018) 1140–1148. doi:10.1016/j.fusengdes.2018.04.090.

[46] J. A. Schwartz, W. Ricks, E. Kolemen, J. Jenkins, Data for the value of fusion energy to a decarbonized United States electric grid. Princeton Plasma Physics Laboratory, Princeton University DataSpace, http://arks.princeton.edu/ark:/88435/dsp012j62s808w.

[47] J. A. Schwartz, W. Ricks, E. Kolemen, J. Jenkins, S. Chakrabarti, N. Patankar, R. Macdonald, Q. Xu, D. S. Mallapragada, P. Monticone, A. Manocha, N. Robinson, GenX v0.2.1 with fusion module, Zenodo (2022). doi:10.5281/zenodo.7507006.

[48] United States Environmental Protection Agency, EPA's Power Sector Modeling Platform v6 using IPM Summer 2021 Reference Case, https://www.epa.gov/power-sector-modeling/epas-power-sector-modeling-platform-v6-using-ipm-summer-2021-reference-case (Sep. 2021).

[49] Z. Selvans, C. Gosnell, A. Sharpe, S. Winter, J. Rousik, E. Welty, B. Norman, PUDL (Nov. 2021). doi:10.5281/zenodo.5677623.

[50] NREL (National Renewable Energy Laboratory), Annual Technology Baseline, Tech. rep., National Renewable Energy Laboratory, Golden, CO (2021).

[51] E. Baik, K. P. Chawla, J. D. Jenkins, C. Kolster, N. S. Patankar, A. Olson, S. M. Benson, J. C. Long, What is different about different net-zero carbon electricity systems?, Energy and Climate Change 2 (2021) 100046. doi:10.1016/j.egycc.2021.100046.

[52] E. Larson, C. Greig, J. Jenkins, E. Mayfield, A. Pascale, C. Zhang, J. Drossman, R. Williams, S. Pacala, R. Socolow, E. Baik, R. Birdsey, R. Duke, R. Jones, B. Haley, E. Leslie, K. Paustian, A. Swan, Net-zero america: Potential pathways, infrastructure, and impacts, Tech. rep., Princeton University, Princeton, NJ (Oct. 2021).

[53] Energy Information Administration, Annual Energy Outlook 2021, https://www.eia.gov/outlooks/archive/aeo21/ (Feb. 2021).

[54] R. Kembleton, C. Bustreo, Prospective research and development for fusion commercialisation, Fusion Engineering and Design 178 (2022) 113069. doi:10.1016/j.fusengdes.2022.113069.

[55] C. Reux, L. Di Gallo, F. Imbeaux, J.-F. Artaud, P. Bernardi, J. Bucalossi, G. Ciraolo, J.-L. Duchateau, C. Fausser, D. Galassi, P. Hertout, J.-C. Jaboulay, A. Li-Puma, B. Saoutic, L. Zani, ITM-TF Contributors, DEMO reactor design using the new modular system code SYCOMORE, Nuclear Fusion 55 (7) (2015) 073011. doi:10.1088/0029-5515/55/7/073011.

[56] S. E. Wurzel, S. C. Hsu, Progress toward Fusion Energy Breakeven and Gain as Measured against the Lawson Criterion, arXiv:2105.10954 [physics] (May 2021). arXiv:2105.10954.